



A new adaptive non-singleton general type-2 fuzzy control of induction motors subject to unknown time-varying dynamics and unknown load torque

Akram Sedaghati¹ · Naser Pariz² · Mehdi Siah³ · Roohollah Barzamini¹

Published online: 5 February 2021

© The Author(s), under exclusive licence to Springer-Verlag GmbH, DE part of Springer Nature 2021

Abstract

In this paper, a new fault-tolerant control strategy is suggested to control the induction motors (IMs). The mathematical model of IMs is supposed to be unknown and also the main disturbances such as perturbation in the rotor resistance, and suddenly changes in the load torque are considered. A general type-2 fuzzy system using a new non-singleton fuzzification is proposed to cope with the uncertainties. The robustness and the stability of the proposed control scheme is studied on basis of the Lyapunov theorem. The simulation results show that the suggested control method has good performance in the versus of unknown dynamics of IM, time-varying disturbances, abrupt faults and measurement errors. The proposed scheme is compared with other popular control systems and other kind of fuzzy systems and singleton fuzzification.

Keywords Induction motor · General type-2 fuzzy systems · Lyapunov stability · Rotor resistance · Load torque

1 Introduction

The induction motor (IMs) is commonly employed in industries because of its reliability, less cost and maintenance free (Deng et al. 2019; Lopes et al. 2017). The dynamics of the induction motors is complicated and is disturbed by variation in rotor resistance and changes in load torque and so on Guedes et al. (2019). Then the control problem of the induction motors has attained great attention in recent years. Various control methods have been applied to the control of IMs. The proposed methods are classified in three categories. In the first category, some simple and ordinary control schemes have been designed for IMs. For instance, the field-oriented control approach is designed for the speed control of IMs (Kubota and Matsuse 1994). In Yu et al. (2001), the vector controller is developed for IMs. The other simple con-

troller which is frequently applied on IMs is PID control method (Lim et al. 2013). Many optimization methods and algorithms have been applied to optimize the PID control for IMs such as genetic algorithm, particle swarm optimization, fuzzy systems, imperialist competitive algorithm and so on (Thangaraj et al. 2011; Ustun and Demirtas 2008; Uddin et al. 2002; Ali 2015).

The next main approach for the control of IMs is the classical control methods. For instance, the predictive control is developed for IMs (Zhang and Yang 2015; Zhang et al. 2016). In Lascau et al. (2016), the feedback linearization method designed for IMs and its performance is compared with the sliding mode approach. The backstepping control technique is studied for IMs in Regaya et al. (2018), and its robustness against variation of rotor resistance is investigated. The immersion and invariance control strategy is studied for IMs in Sabzalian et al. (2019b), and its robustness is investigated. The other most common controller that is frequently used to control of IMs is the sliding model control (SMC) approach. Various version of sliding mode control technique has been studied for IMs such as traditional SMC, adaptive exponential SMC, second-order SMC, terminal SMC, integral SMC, and so on (Xu et al. 2019; Ponce et al. 2018).

The main drawback of the reviewed studies is that the dynamic model of IM is considered to be certain and known. To cope with uncertainties of the mathematical model of

✉ Naser Pariz
n-pariz@um.ac.ir

¹ Department of Electrical Engineering, Central Tehran Branch, Islamic Azad University, Tehran, Iran

² Department of Electrical Engineering, Ferdowsi University of Mashhad, Mashhad, Iran

³ Faculty of Mechanics, Electrical Power and Computer, Science and Research Branch, Islamic Azad University, Tehran, Iran

IM, some intelligent control methods have been proposed (Kalat 2019). In third category, some control approaches have been presented based on the fuzzy systems, neural networks and evolutionary optimization algorithm. For example, in Guazzelli et al. (2018), a predictive controller is designed by genetic algorithm, in which a cost function is minimized to obtain the weighting factors of the conventional predictive controller. The super-twisting technique is employed to improve the field oriented control method (Kali et al. 2018). A simple neuro-fuzzy control method is suggested for IMs, and it is proved that the designed controller has desirable performance in contrast to the conventional PI controller (Gopal and Shivakumar 2019). In Xu et al. (2019), the conventional backstepping strategy is combined with the type-1 fuzzy system to cope with uncertainties. The predictive controller is combined with the Takagi–Sugeno fuzzy system, and it is shown that the performance of the model predictive control is improved (Ammar et al. 2019). The adaptive controller on basis of fuzzy systems, the command filtering and backstepping technique is studied for IMs (Zhao et al. 2018). In Farah et al. (2019), a simple self-evolving fuzzy controller is proposed to improve the performance of indirect field-oriented control scheme. The dynamics of IM is approximated with the fuzzy system in kind of type-1, and then, the feedback controller is designed and its stability is investigated using L_2 optimization (Zina et al. 2018).

In the most of the aforementioned papers, type-1 fuzzy systems and simple neural networks are used to cope with the uncertainties of the dynamics of IMs. Also the robustness of the controller with respect to main faults such as perturbation in the rotor resistance and sudden changes in load torque need more researches. In recent years, it is demonstrated that interval and general type-2 fuzzy systems result in more desirable and more effective performance in approximation of uncertainties (Mohammadzadeh et al. 2019a; Melin et al. 2019; Ontiveros-Robles and Melin 2020; Jana et al. 2019; Zhao et al. 2019). Most recently, the generalized type-2 fuzzy system (GT2FSs) is successfully applied in various applications (Castillo and Atanassov 2019; Castillo et al. 2019). For instance, in Zarandi et al. (2019), GT2FSs are employed for diagnosis of depression. The improved fuzzy systems are used in ship steering systems (Chang et al. 2019). The type-2 fuzzy systems are used to green solid transportation problem (Das et al. 2018). In Sabzalian et al. (2019a), Mohammadzadeh and Kaynak (2019), Jhang et al. (2018), Mohammadzadeh and Zhang (2019) and Mohammadzadeh et al. (2019b) the GT2FSs are used in forecasting and control problems. GT2FSs are used in fault detection and time-series prediction (Boumella et al. 2012; Shabaniyan and Montazeri 2011). Many learning techniques have been suggested to optimize the type-2 fuzzy systems such as bee colony optimization (Zhang et al. 2019), particle swarm optimization (Boumella et al. 2012), among many others. However, the

stable optimization of GT2FSs has been rarely studied. In this paper, the proposed GT2FSs are learned on basis of the tuning laws that are extracted through the robustness analysis.

Based on the aforementioned discussion and motivations, in this study a novel fault-tolerant control scheme is presented. The main innovations of this study are:

1. Unlike the most studies, in this paper dynamic model of IM is considered to be unknown and also it is supposed the dynamics of IM to be disturbed by main faults such as perturbation in the rotor resistance and suddenly changes of load torque.
2. In addition to the dynamic uncertainties and abrupt faults, the effect of measurement errors is also considered.
3. A GT2FS is presented to cope with the uncertainties.
4. The robustness of the suggested control approach is analyzed and a novel compensator is developed to insure the stability and robustness.

The remain structure of this study is as follows. The dynamics of IM is described in Sect. 2. The proposed GT2FS is illustrated in Sect. 3. The control signals and stability analysis are given in Sect. 4. Simulations are presented in Sect. 5, and the conclusion is summarized in Sect. 6.

2 Problem formulation

The mathematical dynamics of the IM are given as:

$$\begin{aligned}
 d\omega/dt &= -n_p T_r/J + \mu\phi_r i_{sq} \\
 d\phi_r/dt &= \frac{M_{sr}}{\tau_r} i_{sd} - \frac{1}{\tau_r} \phi_r \\
 di_{sd}/dt &= \beta\omega\phi_{rq} + \frac{\beta}{\tau_r} \phi_{rd} + \omega_s i_{sq} \\
 &\quad - \frac{1}{\tau_1} i_{sd} + V_{sd}/L_1 \\
 di_{sq}/dt &= -\beta\omega\phi_{rd} + \beta/\tau_r \phi_{rq} - \omega_s i_{sd} \\
 &\quad - \frac{1}{\tau_1} i_{sq} + V_{sq}/L_1
 \end{aligned} \tag{1}$$

where the subscripts q, d, r and s refer to quadrature component, direct component, rotor and stator, respectively. ϕ , V and i , are the flux, voltage and current, respectively. ω represents the rotor speed and ω_s is frequency of stator angular. T_r is the load torque and it is considered to be unknown. The other parameters are defined as follows:

$$\begin{aligned}
 \tau_r &= L_r/R_r \\
 L_1 &= L_s - \frac{M_{sr}^2}{L_r} \\
 R_1 &= R_s + R_r \left(\frac{M_{sr}}{L_r} \right)^2 \\
 \beta &= \frac{M_{sr}}{L_r L_1}
 \end{aligned}$$

$$\begin{aligned} \mu &= n_p^2 \left(\frac{M_{sr}}{JL_r} \right) \\ \tau_1 &= \frac{L_1}{R_1} \end{aligned} \tag{2}$$

where J express moment of inertia, the number of pole pairs is represented by n_p , L_r/L_s is the rotor/stator inductances, R_r/R_s is the rotor/stator resistance and M_{sr} represents the mutual inductance.

The dynamics of IM in (1) are rewritten as follows:

$$\begin{aligned} \dot{y}_1 &= y_4 + f_1(y) \\ \dot{y}_2 &= y_3 + f_2(y) \\ \dot{y}_3 &= \frac{1}{L_1}u_1 + f_3(y) \\ \dot{y}_4 &= \frac{1}{L_1}u_2 + f_4(y) \end{aligned} \tag{3}$$

where

$$\begin{aligned} f_1(y) &= -\frac{n_p T_r}{J} - i_{sq} + \mu \phi_r i_{sq} \\ f_2(y) &= \frac{M_{sr}}{\tau_r} i_{sd} - i_{sd} - \frac{1}{\tau_r} \phi_r \\ f_3(y) &= -\frac{1}{\tau_1} i_{sd} + \omega_s i_{sq} \frac{\beta}{\tau_r} \phi_r \\ f_4(y) &= -\frac{1}{\tau_1} i_{sq} - \beta \omega \phi_r - \omega_s i_{sd} \end{aligned} \tag{4}$$

$$\begin{aligned} u_1 &= V_{sd}, \quad u_2 = V_{sq}, \quad y_1 = \omega, \quad y_2 = \phi_r, \\ y_3 &= i_{sd}, \quad y_4 = i_{sq}, \quad \underline{y} = [y_1, \dots, y_4]^T \end{aligned} \tag{5}$$

By using the suggested GT2FS, the dynamics of IM in (3) are online estimated as follows:

$$\begin{aligned} \hat{y}_1 &= \hat{y}_4 + \hat{f}_1(\hat{y}|\theta_1) \\ \hat{y}_2 &= \hat{y}_3 + \hat{f}_2(\hat{y}|\theta_2) \\ \hat{y}_3 &= \hat{f}_3(\hat{y}|\theta_3) + \frac{1}{L_1}u_1 \\ \hat{y}_4 &= \hat{f}_4(\hat{y}|\theta_4) + \frac{1}{L_1}u_2 \end{aligned} \tag{6}$$

where $\hat{f}_i, i = 1, \dots, 4$ are the suggested GT2GSs and $\hat{y} = [\hat{y}_1, \dots, \hat{y}_4]^T$. $\hat{f}_1, \hat{f}_2, \hat{f}_3$ and \hat{f}_4 are the estimation of $f_1(y), f_2(y), f_3(y)$ and $f_4(y)$, respectively. A general view on the proposed control scheme shown in Fig. 1.

3 Suggested fuzzy system

In this section, the suggested GT2FS is explained. The suggested structure is displayed in Fig. 2. Consider the i th GT2FS, the details are described in below.

1. The estimated states $\hat{y}_k, k = 1, \dots, 4$ are the inputs of GT2FS \hat{f}_i .
2. Consider the n th membership function (MF) for the k th input as \tilde{A}_k^n ; by conventional singleton fuzzification, the upper membership and the lower membership of \tilde{A}_k^n at

Fig. 1 The general view on the suggested controller

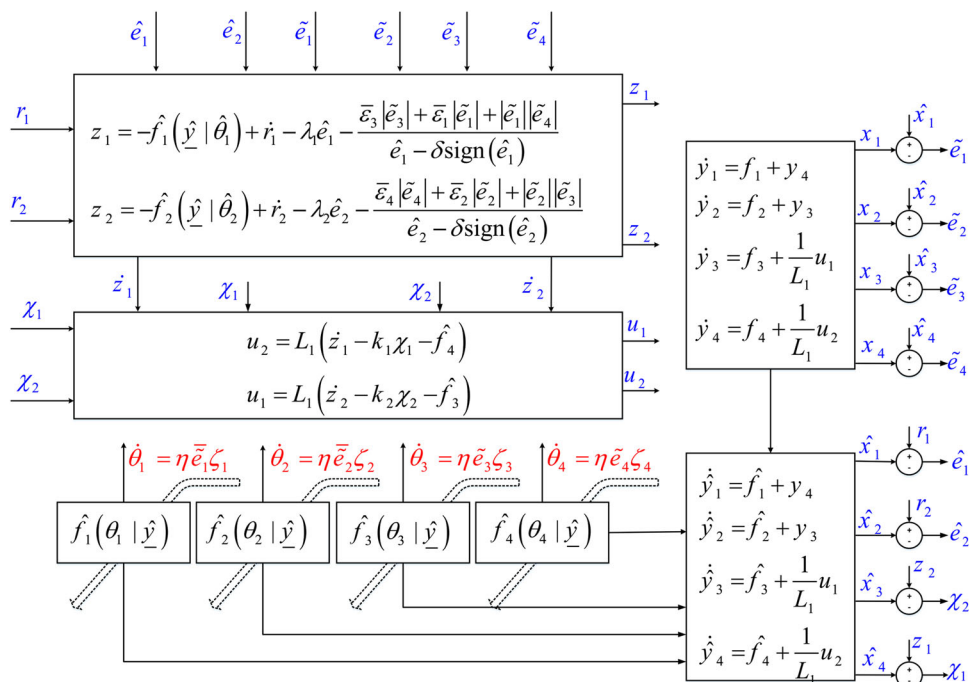
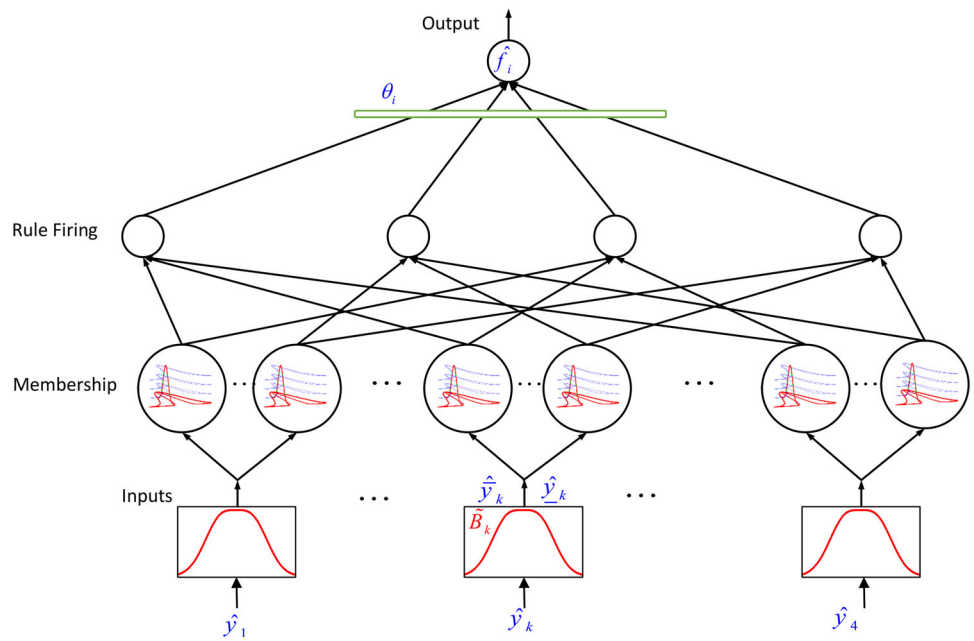


Fig. 2 The structure of the generalized type-2 fuzzy system



the horizontal slice level α are computed as follows:

$$\begin{aligned} \bar{\mu}_{k|\alpha}^n &= \exp\left(-\frac{(\hat{y}_k - c_{\tilde{A}_k^n})^2}{\bar{\sigma}_{\tilde{A}_k|\alpha}^2}\right) \\ \underline{\mu}_{k|\alpha}^n &= \exp\left(-\frac{(\hat{y}_k - c_{\tilde{A}_k^n})^2}{\underline{\sigma}_{\tilde{A}_k|\alpha}^2}\right) \end{aligned} \quad (7)$$

where $c_{\tilde{A}_k^n}$, $\bar{\sigma}_{\tilde{A}_k|\alpha}^n$ and $\underline{\sigma}_{\tilde{A}_k|\alpha}^n$, express the center, upper standard division and lower standard division of the Gaussian MF $\tilde{A}_{k|\alpha}^n$, respectively. \hat{y}_k is the k -th input. $\bar{\mu}_{k|\alpha}^n$ and $\underline{\mu}_{k|\alpha}^n$ are the upper and lower membership of \tilde{A}_k^n . By the proposed non-singleton fuzzification, the upper membership and the lower membership of \tilde{A}_k^n at the hor-

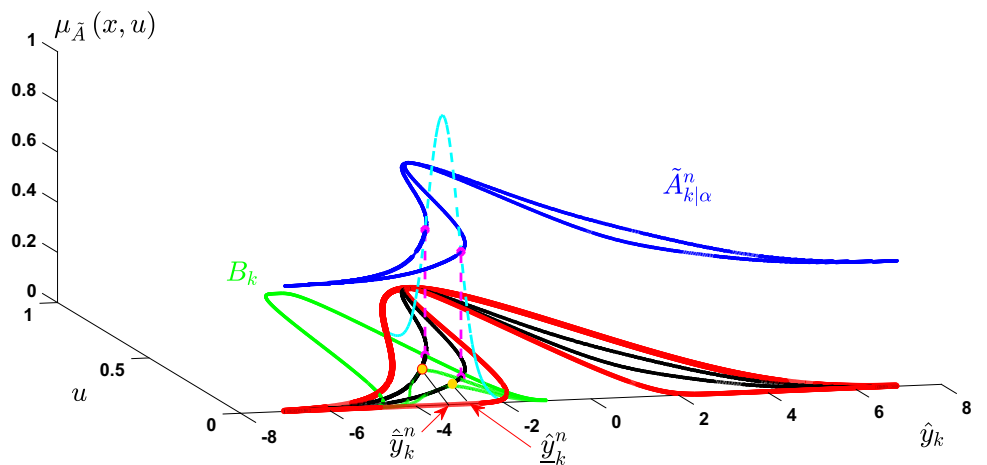
izontal slice level α are computed as follows:

$$\begin{aligned} \bar{\mu}_{k|\alpha}^n &= \exp\left(-\frac{(\hat{y}_k^n - c_{\tilde{A}_k^n})^2}{\bar{\sigma}_{\tilde{A}_k|\alpha}^2}\right) \\ \underline{\mu}_{k|\alpha}^n &= \exp\left(-\frac{(\hat{y}_k^n - c_{\tilde{A}_k^n})^2}{\underline{\sigma}_{\tilde{A}_k|\alpha}^2}\right) \end{aligned} \quad (8)$$

where \hat{y}_k^n and $\underline{\hat{y}}_k^n$ are computed as (see Fig. 3):

$$\hat{y}_k^n = \frac{\sigma_{B_k}^2 c_{\tilde{A}_i^n} + \bar{\sigma}_{\tilde{A}_k|\alpha}^2 \hat{y}_k}{\sigma_{B_k}^2 c_{\tilde{A}_i^n} + \bar{\sigma}_{\tilde{A}_k|\alpha}^2 \hat{y}_k} \quad (9)$$

Fig. 3 The proposed non-singleton fuzzification



$$\hat{y}_k^n = \frac{\sigma_{B_k}^2 c_{A_i^j} + \sigma_{A_{k|\alpha}^n}^2 \hat{y}_k}{\sigma_{B_k}^2 c_{A_i^j} + \sigma_{A_{k|\alpha}^n}^2 \hat{y}_k} \tag{10}$$

where σ_{B_k} is a parameter in the membership function B_k for k th input. The membership of B_k is obtained as:

$$\mu_{B_k} = \left[1 + \frac{(y - \hat{y}_k)^2}{\sigma_{B_k}^2} \right] \exp \left[-\frac{(y - \hat{y}_k)^2}{\sigma_{B_k}^2} \right] \tag{11}$$

3. The rule firing are obtained as follows:

$$\begin{aligned} \bar{\psi}_{n|\alpha} &= \bar{\mu}_{1|\alpha}^n \times \dots \times \bar{\mu}_{4|\alpha}^n \\ \underline{\psi}_{n|\alpha} &= \underline{\mu}_{1|\alpha}^n \times \dots \times \underline{\mu}_{4|\alpha}^n \end{aligned} \tag{12}$$

where $\bar{\psi}_{n|\alpha}$ and $\underline{\psi}_{n|\alpha}$ represent upper rule firing and lower rule firing of n th rule at level α -cut.

4. On the basis of the Nie-Tan type-reduction (Fekih 2008), one has:

$$f_i = \sum_{j=1}^{N_\alpha} \alpha_j \theta_i^T \xi_{i|\alpha_j} / \sum_{j=1}^{N_\alpha} \alpha_j \tag{13}$$

$$\begin{aligned} \xi_{i|\alpha_j} &= \frac{1}{\sum_{n=1}^{N_r} \bar{\psi}_{n|\alpha_j} + \underline{\psi}_{n|\alpha_j}} \\ & \left[\bar{\psi}_{1|\alpha_j} + \underline{\psi}_{1|\alpha_j}, \dots, \bar{\psi}_{N_r|\alpha_j} + \underline{\psi}_{N_r|\alpha_j} \right]^T \end{aligned} \tag{14}$$

where \hat{f}_i is the output, N_r represents the rule numbers, N_α is the number of α -cuts and θ_i is the vector of the consequent parameters. f_i can be rewritten as follows:

$$f_i = \theta_i^T \zeta_i \tag{15}$$

where

$$\zeta_i = \sum_{j=1}^{N_\alpha} \xi_{i|\alpha_j} / \sum_{j=1}^{N_\alpha} \alpha_j \tag{16}$$

4 Main results

The main outcomes of the study are given in the following theorem.

Theorem 1 *The system (3) is stable, asymptotically, if the controllers and the tuning rules of the fuzzy systems are designed as follows:*

$$\frac{1}{L_1} u_2 = \dot{z}_1 - k_1 \chi_1 - \hat{f}_4$$

$$\frac{1}{L_1} u_1 = \dot{z}_2 - k_2 \chi_2 - \hat{f}_3 \tag{17}$$

$$\begin{aligned} \dot{\theta}_1 &= \eta \tilde{e}_1 \zeta_1 \\ \dot{\theta}_2 &= \eta \tilde{e}_2 \zeta_2 \\ \dot{\theta}_3 &= \eta \tilde{e}_3 \zeta_3 \\ \dot{\theta}_4 &= \eta \tilde{e}_4 \zeta_4 \end{aligned} \tag{18}$$

where k_1 and k_2 are constants with positive values and the variables $\chi_i, z_i, i = 1, 2$ are defined as follows:

$$\chi_2 = \hat{y}_3 - z_2 \quad \chi_1 = \hat{y}_4 - z_1 \tag{19}$$

$$\begin{aligned} z_1 &= -\hat{f}_1(\hat{y}|\theta_1) + \dot{r}_1 - \lambda_1 \hat{e}_1 \\ & \quad - (\bar{\epsilon}_3 |\tilde{e}_3| + \bar{\epsilon}_1 |\tilde{e}_1| + \bar{\epsilon}_1 |\tilde{e}_4|) / (\hat{e}_1 - \delta \text{sign}(\hat{e}_1)) \end{aligned} \tag{20}$$

$$\begin{aligned} z_2 &= -\hat{f}_2(\hat{y}|\theta_2) + \dot{r}_2 - \lambda_2 \hat{e}_2 \\ & \quad - (\bar{\epsilon}_4 |\tilde{e}_4| + \bar{\epsilon}_2 |\tilde{e}_2| + \bar{\epsilon}_2 |\tilde{e}_3|) / (\hat{e}_2 - \delta \text{sign}(\hat{e}_2)) \end{aligned}$$

where $\hat{f}_i(\hat{y}|\theta_i), i = 1, \dots, 4$ are proposed fuzzy system, r_1 and r_2 are the reference signals, λ_1 and λ_2 are constant variables with the positive values, δ is small positive constant, \hat{e}_i and $\tilde{e}_i, i = 1, \dots, 4$ are defined as $\hat{e}_i = \hat{y}_i - r_i, \tilde{e}_i = y_i - \hat{y}_i, \bar{\epsilon}_i, i = 1, \dots, 4$ are the upper bounds of ϵ_i where are defined as follows:

$$\begin{aligned} \epsilon_1 &= \left[f_1(\underline{y}) - \hat{f}_1^*(\hat{y}|\theta_1^*) \right] \\ \epsilon_2 &= \left[f_2(\underline{y}) - \hat{f}_2^*(\hat{y}|\theta_2^*) \right] \\ \epsilon_3 &= \left[f_3(\underline{y}) - \hat{f}_3^*(\hat{y}|\theta_3^*) \right] \\ \epsilon_4 &= \left[f_4(\underline{y}) - \hat{f}_4^*(\hat{y}|\theta_4^*) \right] \end{aligned} \tag{21}$$

where $\hat{f}_i^*(\hat{y}|\theta_i^*), i = 1, \dots, 4$ are the proposed type-2 fuzzy system with optimal parameters θ_i^* . Also $\tilde{\theta}_i, i = 1, \dots, 4$ are defined as:

$$\begin{aligned} \tilde{\theta}_1 &= \theta_1^* - \theta_1 \\ \tilde{\theta}_2 &= \theta_2^* - \theta_2 \\ \tilde{\theta}_3 &= \theta_3^* - \theta_3 \\ \tilde{\theta}_4 &= \theta_4^* - \theta_4 \end{aligned} \tag{22}$$

Proof Substituting (20) into (6), yields:

$$\begin{aligned} \dot{\hat{e}}_1 &= -\lambda_1 \hat{e}_1 \\ & \quad - (\bar{\epsilon}_3 |\tilde{e}_3| + \bar{\epsilon}_1 |\tilde{e}_1| + |\tilde{e}_1| |\tilde{e}_4|) / (\hat{e}_1 - \delta \text{sign}(\hat{e}_1)) \\ \dot{\hat{e}}_2 &= -\lambda_2 \hat{e}_2 \\ & \quad - (\bar{\epsilon}_4 |\tilde{e}_4| + \bar{\epsilon}_2 |\tilde{e}_2| + |\tilde{e}_2| |\tilde{e}_3|) / (\hat{e}_2 - \delta \text{sign}(\hat{e}_2)) \end{aligned} \tag{23}$$

The dynamics of $\tilde{e}_1, \tilde{e}_2, \tilde{e}_3$ and \tilde{e}_4 are obtained as follows:

$$\begin{aligned} \dot{\tilde{e}}_1 &= \hat{f}_1^* (\hat{y}|\theta_1^*) - \hat{f}_1 (\hat{y}|\theta_1) + \left[f_1 (\underline{y}) - \hat{f}_1^* (\hat{y}|\theta_1^*) \right] + \tilde{e}_4 \\ \dot{\tilde{e}}_2 &= \hat{f}_2^* (\hat{y}|\theta_2^*) - \hat{f}_2 (\hat{y}|\theta_2) + \left[f_2 (\underline{y}) - \hat{f}_2^* (\hat{y}|\theta_2^*) \right] + \tilde{e}_3 \\ \dot{\tilde{e}}_3 &= \hat{f}_3^* (\hat{y}|\theta_3^*) - \hat{f}_3 (\hat{y}|\theta_3) + \left[f_3 (\underline{y}) - \hat{f}_3^* (\hat{y}|\theta_3^*) \right] \\ \dot{\tilde{e}}_4 &= \hat{f}_4^* (\hat{y}|\theta_4^*) - \hat{f}_4 (\hat{y}|\theta_4) + \left[f_4 (\underline{y}) - \hat{f}_4^* (\hat{y}|\theta_4^*) \right] \end{aligned} \tag{24}$$

By substituting (21) into equation (24), one has:

$$\begin{aligned} \dot{\tilde{e}}_1 &= \tilde{\theta}_1^T \zeta_1 + \varepsilon_1 + \tilde{e}_4 \\ \dot{\tilde{e}}_2 &= \tilde{\theta}_2^T \zeta_2 + \varepsilon_2 + \tilde{e}_3 \\ \dot{\tilde{e}}_3 &= \tilde{\theta}_3^T \zeta_3 + \varepsilon_3 \\ \dot{\tilde{e}}_4 &= \tilde{\theta}_4^T \zeta_4 + \varepsilon_4 \end{aligned} \tag{25}$$

Time derivative of χ_2 and χ_1 in (19), are obtained as follows:

$$\begin{aligned} \dot{\chi}_1 &= \hat{f}_4 + \frac{1}{L_1} u_2 - \dot{z}_1 \\ \dot{\chi}_2 &= \hat{f}_3 + \frac{1}{L_1} u_1 - \dot{z}_2 \end{aligned} \tag{26}$$

From (17) and (26), the dynamics of χ_1 and χ_2 can be written as follows:

$$\begin{aligned} \dot{\chi}_1 &= -k_1 \chi_1 \\ \dot{\chi}_2 &= -k_2 \chi_2 \end{aligned} \tag{27}$$

To prove the closed-loop stability, the following Lyapunov function is considered:

$$\begin{aligned} V &= \frac{1}{2} \hat{e}_1^2 + \frac{1}{2} \hat{e}_2^2 + \frac{1}{2} \tilde{e}_1^2 + \frac{1}{2} \tilde{e}_2^2 + \frac{1}{2} \tilde{e}_3^2 + \frac{1}{2} \tilde{e}_4^2 + \frac{1}{2} \chi_1^2 + \frac{1}{2} \chi_2^2 \\ &+ \frac{1}{2\eta} \tilde{\theta}_1^T \tilde{\theta}_2 + \frac{1}{2\eta} \tilde{\theta}_2^T \tilde{\theta}_2 + \frac{1}{2\eta} \tilde{\theta}_3^T \tilde{\theta}_3 + \frac{1}{2\eta} \tilde{\theta}_4^T \tilde{\theta}_4 \end{aligned} \tag{28}$$

where η is the tuning rate. By taking time derivative of (28), one has:

$$\begin{aligned} \dot{V} &= \hat{e}_1 \dot{\hat{e}}_1 + \hat{e}_2 \dot{\hat{e}}_2 + \tilde{e}_1 \dot{\tilde{e}}_1 + \tilde{e}_2 \dot{\tilde{e}}_2 + \tilde{e}_3 \dot{\tilde{e}}_3 + \tilde{e}_4 \dot{\tilde{e}}_4 \\ &+ \chi_1 \dot{\chi}_1 + \chi_2 \dot{\chi}_2 - \frac{1}{\eta} \tilde{\theta}_1^T \dot{\tilde{\theta}}_1 - \frac{1}{\eta} \tilde{\theta}_2^T \dot{\tilde{\theta}}_2 \\ &- \frac{1}{\eta} \tilde{\theta}_3^T \dot{\tilde{\theta}}_3 - \frac{1}{\eta} \tilde{\theta}_4^T \dot{\tilde{\theta}}_4 \end{aligned} \tag{29}$$

Substituting $\dot{\hat{e}}_1$ and $\dot{\hat{e}}_2$ from (23), $\dot{\tilde{e}}_i$ $i = 1, \dots, 4$ from (25) and $\dot{\chi}_1$ and $\dot{\chi}_2$ from (27), yields:

$$\dot{V} = \hat{e}_1 \left[-\lambda_1 \hat{e}_1 - \frac{\bar{\varepsilon}_3 |\tilde{e}_3| + \bar{\varepsilon}_1 |\tilde{e}_1| + |\tilde{e}_1| |\tilde{e}_4|}{\hat{e}_1 - \delta \text{sign}(\hat{e}_1)} \right]$$

$$\begin{aligned} &+ \hat{e}_2 \left[-\lambda_2 \hat{e}_2 - \frac{\bar{\varepsilon}_4 |\tilde{e}_4| + \bar{\varepsilon}_2 |\tilde{e}_2| + |\tilde{e}_2| |\tilde{e}_3|}{\hat{e}_2 - \delta \text{sign}(\hat{e}_2)} \right] \\ &+ \tilde{e}_1 \left(\tilde{\theta}_1^T \zeta_1 + \varepsilon_1 + \tilde{e}_4 \right) + \tilde{e}_2 \left(\tilde{\theta}_2^T \zeta_2 + \varepsilon_2 + \tilde{e}_3 \right) \\ &+ \tilde{e}_3 \left(\tilde{\theta}_3^T \zeta_3 + \varepsilon_3 \right) + \tilde{e}_4 \left(\tilde{\theta}_4^T \zeta_4 + \varepsilon_4 \right) \\ &+ \chi_1 (-k_1 \chi_1) + \chi_2 (-k_2 \chi_2) \\ &- \frac{1}{\eta} \tilde{\theta}_1^T \dot{\tilde{\theta}}_1 - \frac{1}{\eta} \tilde{\theta}_2^T \dot{\tilde{\theta}}_2 \\ &- \frac{1}{\eta} \tilde{\theta}_3^T \dot{\tilde{\theta}}_3 - \frac{1}{\eta} \tilde{\theta}_4^T \dot{\tilde{\theta}}_4 \end{aligned} \tag{30}$$

Equation (30) can be rewritten as follows:

$$\begin{aligned} \dot{V} &= -\lambda_1 \hat{e}_1^2 - \lambda_2 \hat{e}_2^2 - k_1 \chi_1^2 - k_2 \chi_2^2 \\ &+ (\varepsilon_1 \tilde{e}_1 + \tilde{e}_1 \tilde{e}_4 + \varepsilon_3 \tilde{e}_3) \\ &- \hat{e}_1 (\bar{\varepsilon}_3 |\tilde{e}_3| + \bar{\varepsilon}_1 |\tilde{e}_1| + |\tilde{e}_1| |\tilde{e}_4|) / (\hat{e}_1 - \delta \text{sign}(\hat{e}_1)) \\ &+ (\varepsilon_2 \tilde{e}_2 + \tilde{e}_2 \tilde{e}_3 + \varepsilon_4 \tilde{e}_4) \\ &- \hat{e}_2 (\bar{\varepsilon}_4 |\tilde{e}_4| + \bar{\varepsilon}_2 |\tilde{e}_2| + |\tilde{e}_2| |\tilde{e}_3|) / (\hat{e}_2 - \delta \text{sign}(\hat{e}_2)) \\ &+ \tilde{e}_1 \tilde{\theta}_1^T \zeta_1 - \frac{1}{\eta} \tilde{\theta}_1^T \dot{\tilde{\theta}}_1 + \tilde{e}_2 \tilde{\theta}_2^T \zeta_2 - \frac{1}{\eta} \tilde{\theta}_2^T \dot{\tilde{\theta}}_2 \\ &+ \tilde{e}_3 \tilde{\theta}_3^T \zeta_3 - \frac{1}{\eta} \tilde{\theta}_3^T \dot{\tilde{\theta}}_3 + \tilde{e}_4 \tilde{\theta}_4^T \zeta_4 - \frac{1}{\eta} \tilde{\theta}_4^T \dot{\tilde{\theta}}_4 \end{aligned} \tag{31}$$

Substituting the adaptation laws of θ_i , $i = 3, 4$ from (18) into (31), results in:

$$\begin{aligned} \dot{V} &= -\lambda_1 \hat{e}_1^2 - \lambda_2 \hat{e}_2^2 - k_1 \chi_1^2 - k_2 \chi_2^2 \\ &+ (\varepsilon_1 \tilde{e}_1 + \tilde{e}_1 \tilde{e}_4 + \varepsilon_3 \tilde{e}_3) \\ &- \hat{e}_1 (\bar{\varepsilon}_3 |\tilde{e}_3| + \bar{\varepsilon}_1 |\tilde{e}_1| + |\tilde{e}_1| |\tilde{e}_4|) / (\hat{e}_1 - \delta \text{sign}(\hat{e}_1)) \\ &+ (\varepsilon_2 \tilde{e}_2 + \tilde{e}_2 \tilde{e}_3 + \varepsilon_4 \tilde{e}_4) \\ &- \hat{e}_2 (\bar{\varepsilon}_4 |\tilde{e}_4| + \bar{\varepsilon}_2 |\tilde{e}_2| + |\tilde{e}_2| |\tilde{e}_3|) / (\hat{e}_2 - \delta \text{sign}(\hat{e}_2)) \end{aligned} \tag{32}$$

From (32), one has:

$$\begin{aligned} \dot{V} &\leq -\lambda_1 \hat{e}_1^2 - \lambda_2 \hat{e}_2^2 - k_1 \chi_1^2 - k_2 \chi_2^2 \\ &+ (|\varepsilon_1| |\tilde{e}_1| + |\tilde{e}_1 \tilde{e}_4| + |\varepsilon_3| |\tilde{e}_3|) \\ &- \hat{e}_1 (\bar{\varepsilon}_3 |\tilde{e}_3| + \bar{\varepsilon}_1 |\tilde{e}_1| + |\tilde{e}_1| |\tilde{e}_4|) / (\hat{e}_1 - \delta \text{sign}(\hat{e}_1)) \\ &+ (|\varepsilon_2| |\tilde{e}_2| + |\tilde{e}_2 \tilde{e}_3| + |\varepsilon_4| |\tilde{e}_4|) \\ &- \hat{e}_2 (\bar{\varepsilon}_4 |\tilde{e}_4| + \bar{\varepsilon}_2 |\tilde{e}_2| + |\tilde{e}_2| |\tilde{e}_3|) / (\hat{e}_2 - \delta \text{sign}(\hat{e}_2)) \end{aligned} \tag{33}$$

From (33) and considering the fact that:

$$\begin{aligned} \hat{e}_1 / (\hat{e}_1 - \delta \text{sign}(\hat{e}_1)) &\geq 1 \\ \hat{e}_2 / (\hat{e}_2 - \delta \text{sign}(\hat{e}_2)) &\geq 1 \end{aligned} \tag{34}$$

One has:

$$\begin{aligned} (|\varepsilon_1| |\tilde{e}_1| + |\tilde{e}_1 \tilde{e}_4| + |\varepsilon_3| |\tilde{e}_3|) - \\ \hat{e}_1 (\bar{\varepsilon}_3 |\tilde{e}_3| + \bar{\varepsilon}_1 |\tilde{e}_1| + |\tilde{e}_1| |\tilde{e}_4|) / (\hat{e}_1 - \delta \text{sign}(\hat{e}_1)) &\leq 0 \\ (|\varepsilon_2| |\tilde{e}_2| + |\tilde{e}_2 \tilde{e}_3| + |\varepsilon_4| |\tilde{e}_4|) - \\ \hat{e}_2 (\bar{\varepsilon}_4 |\tilde{e}_4| + \bar{\varepsilon}_2 |\tilde{e}_2| + |\tilde{e}_2| |\tilde{e}_3|) / (\hat{e}_2 - \delta \text{sign}(\hat{e}_2)) &\leq 0 \end{aligned} \tag{35}$$

From (35), the inequality (33), becomes:

$$\dot{V} \leq -\lambda_1 \hat{e}_1^2 - \lambda_2 \hat{e}_2^2 - k_1 \chi_1^2 - k_2 \chi_2^2 \tag{36}$$

Since the $\hat{e}_1, \hat{e}_2, \chi_1$ and χ_2 are limited, then \dot{V} is bounded and then on the basis Barbalat's lemma the asymptotic stability is proved and the proof is completed. \square

5 Simulation

This section presents the examination of the performance of the designed control scheme on an induction motor by 1.5 kW cage rotor and (220–380 V) power supply. The parameters of simulation are given in Tables 1 and 2. The performance of the suggested controller is evaluated in three scenarios, and finally a comparison with other popular control techniques is presented.

Scenario 1 In the first scenario, it is assumed that there is no fault but the dynamics of IM is unknown. The trajectory of output y_1 (rotor speed) is shown in Fig. 4 and the trajectory

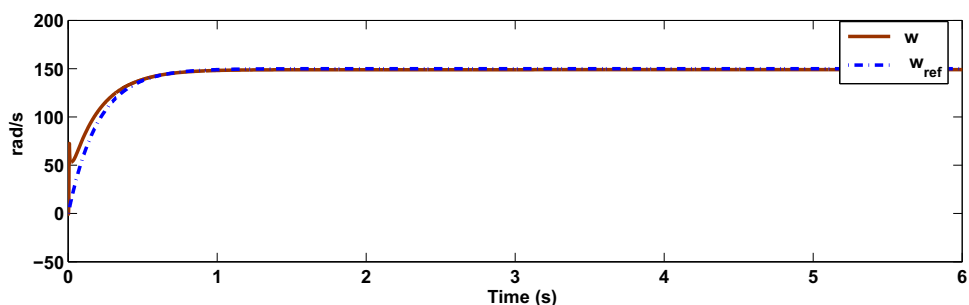
Table 1 The IM parameters

Parameter	Description	Value	Units
R_r	Rotor resistance	1	Ω
R_s	Stator resistance	1.2	Ω
L_r	Rotor inductance	0.1568	H
L_s	Stator inductance	0.1554	H
–	Rated speed	1480	rpm
T_{rN}	Rated load	5	N_m
n_p	Number of pole pairs	2	–
M_{sr}	Mutual inductance	0.15	H
J	Rotor inertia	0.013	$kg\ m^2$

Table 2 The simulation parameters

$\lambda_i, i = 1, 2$	$k_i, i = 1, 2$	δ	η	$\bar{\varepsilon}_i, i = 1, \dots, 4$
See (20)	See (17)	See (23)	See (18)	See (21)
20	20	0.01	0.1	100

Fig. 4 Scenario 1: the tracking performance of rotor speed



of the second output y_2 (rotor flux) is depicted in Fig. 5. The tracking errors e_1 and e_2 are shown in Figs. 6 and 7, respectively. The trajectories of the direct component and the quadrature component of the stator current are given in Figs. 8 and 9, respectively. The direct component and the quadrature component of the control signals are provided in Figs. 10 and 11. One can see that the trajectories of y_1 and y_2 are well reached to the reference values in a finite time.

Scenario 2 In second scenario in addition to the fact that dynamics of IM is unknown, the main faults, such as perturbation in the rotor resistance and sudden changes of load torque, are considered as below. The perturbation of the rotor resistance is considered as $R_r = R_{rN} (2 - \exp(-1.5t))$, where R_{rN} represents the nominal case of R_r and the load torque is assumed to be suddenly changed from (5 N_m) at $t = 3$ s as depicted in Fig. 12. The rotor speed y_1 is given in Fig. 13, and the trajectory of the second output y_2 (rotor flux) is depicted in Fig. 14. The tracking errors e_1 and e_2 are shown in Figs. 15 and 16, respectively. The trajectories of the stator current (direct component and the quadrature component) are given in Figs. 17 and 18. The direct/quadrature component of input voltage is displayed in Fig. 19/Fig. 20. One can see that the proposed controller could overcome the changes of the load torque, and variation of rotor resistance and the trajectories of rotor speed y_1 and rotor flux y_2 well track the desired reference under faulty conditions.

Scenario 3 In third scenario in addition to the unknown dynamics of IM and presence of the main faults such as considered in Scenario 2, the measurement errors are also considered. The measurement errors are considered to white noise that are added to the output signals. The results are given in Table 3. One can see that the proposed controller using GT2FS and non-singleton fuzzification could better overcome the measurement errors, changes of the load torque and variation of rotor resistance, in contrast to T1FS, IT2FS and singleton fuzzification.

Comparison To demonstrate the capability of the suggested controller, a comparison with the other control techniques is provided. The control methods such as the fault tolerant control method (FTAC) (Fekih 2008), field oriented control approach (FOC) (Fekih 2008), the adaptive sliding mode controller (ASMC) (Dong et al. 2016) and type-2 fuzzy sliding

Fig. 5 Scenario 1: the tracking performance of rotor flux

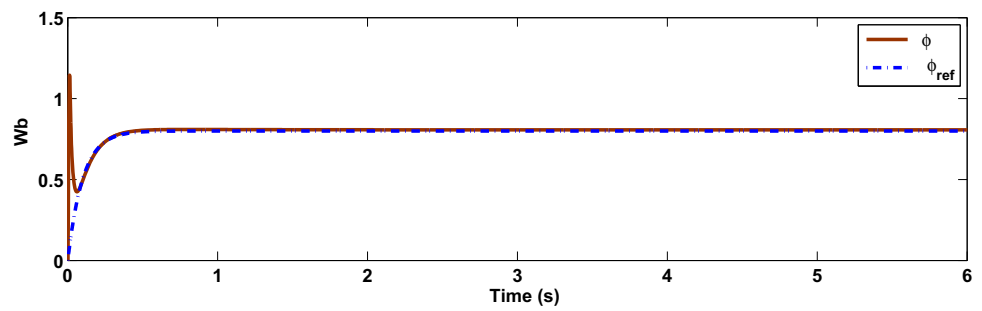


Fig. 6 Scenario 1: the trajectory of the tracking error (rotor speed)

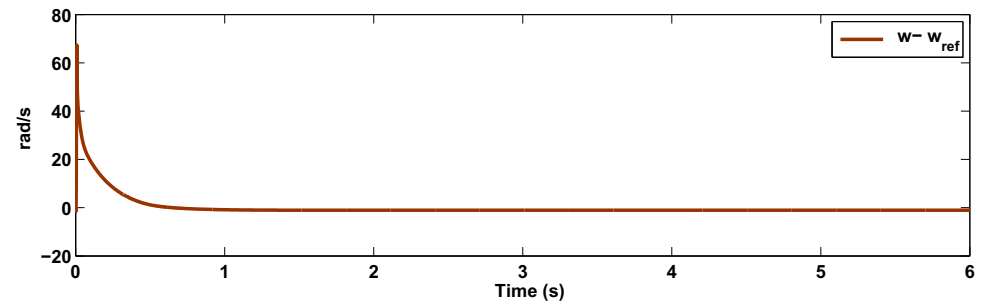


Fig. 7 Scenario 1: the trajectory of the tracking error (rotor flux)

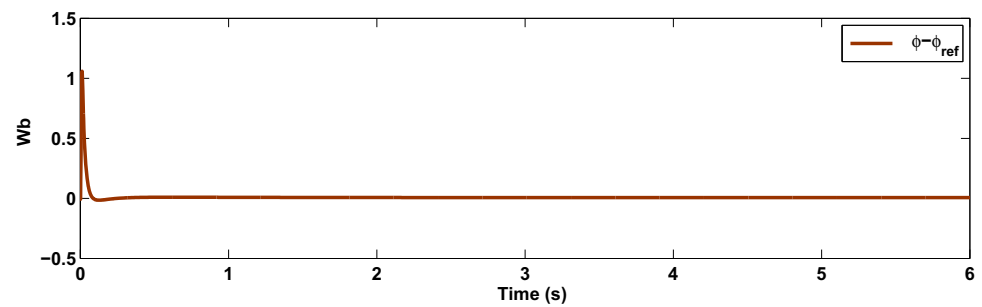


Fig. 8 Scenario 1: the stator current (direct component)

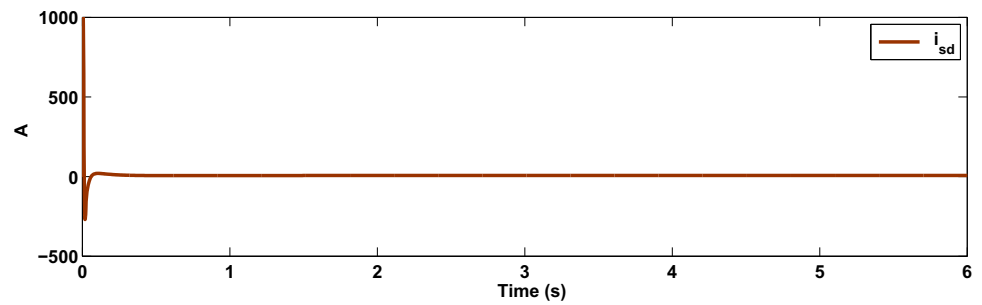


Fig. 9 Scenario 1: the stator current (quadrature component)

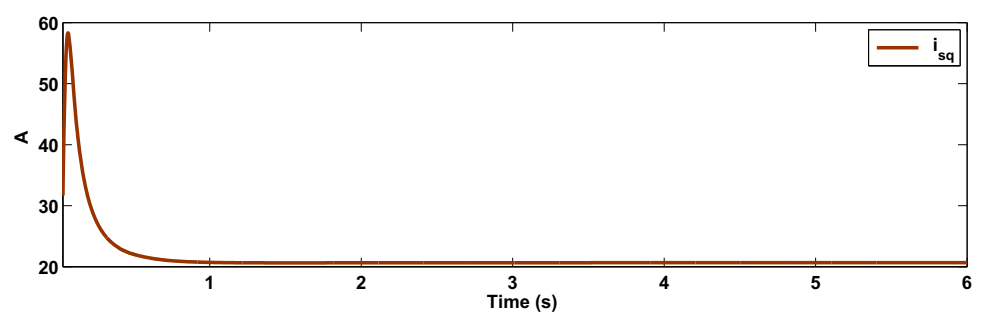


Fig. 10 Scenario 1: the control signal (V_{sd})

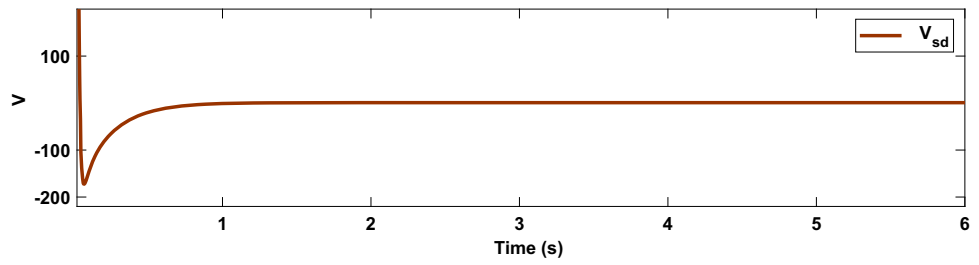


Fig. 11 Scenario 1: the control signal (V_{sq})

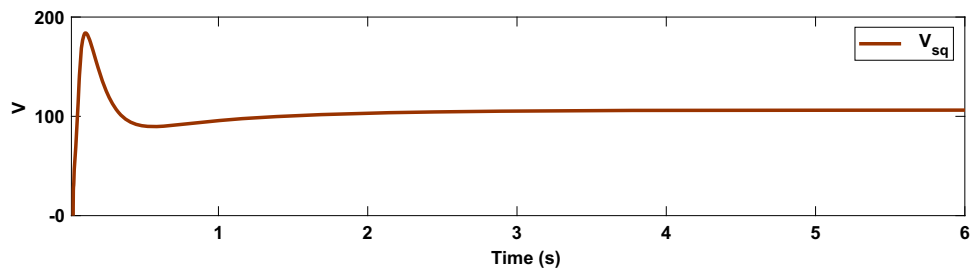


Fig. 12 Scenario 2: the variation of the load torque

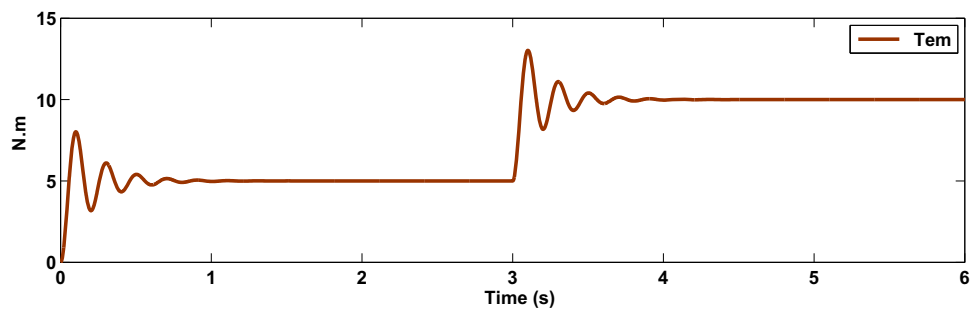


Fig. 13 Scenario 2: the tracking performance of rotor speed

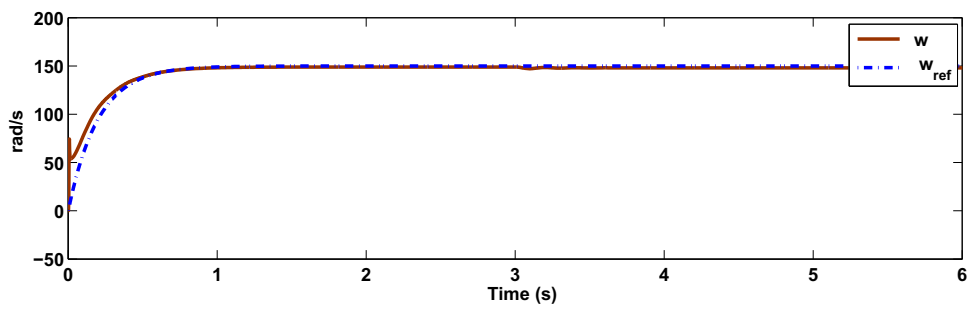


Fig. 14 Scenario 2: the tracking performance of rotor flux

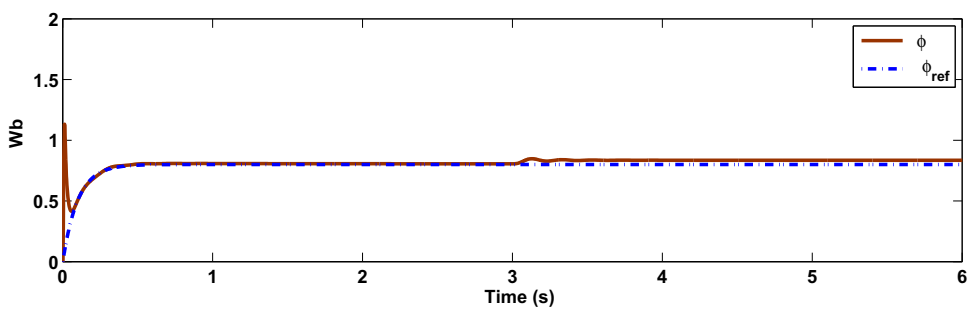


Fig. 15 Scenario 2: the trajectory of the tracking error of the rotor speed

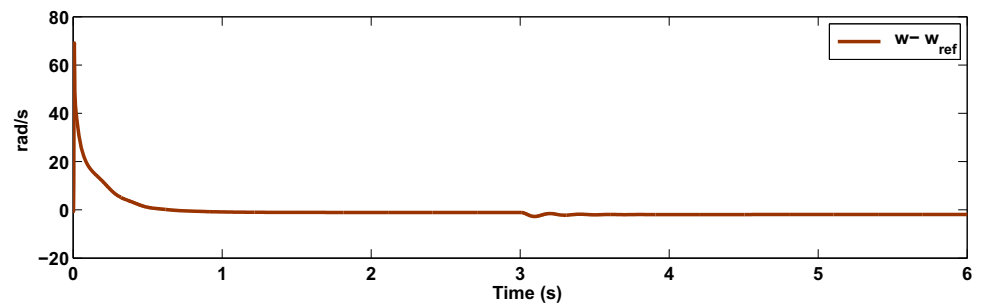


Fig. 16 Scenario 2: the trajectory of the tracking error (rotor flux)

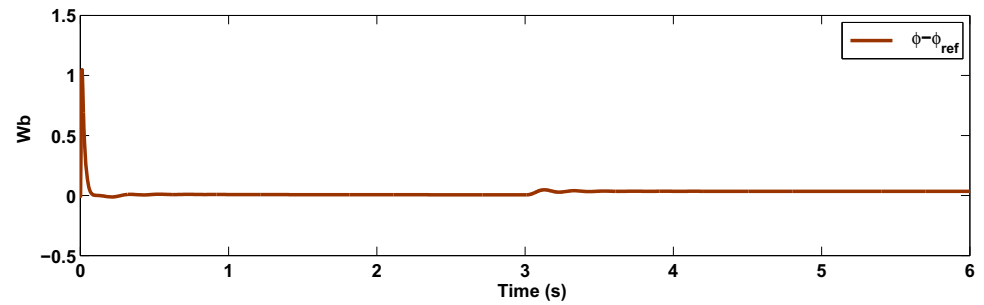


Fig. 17 Scenario 2: the stator current (direct component)

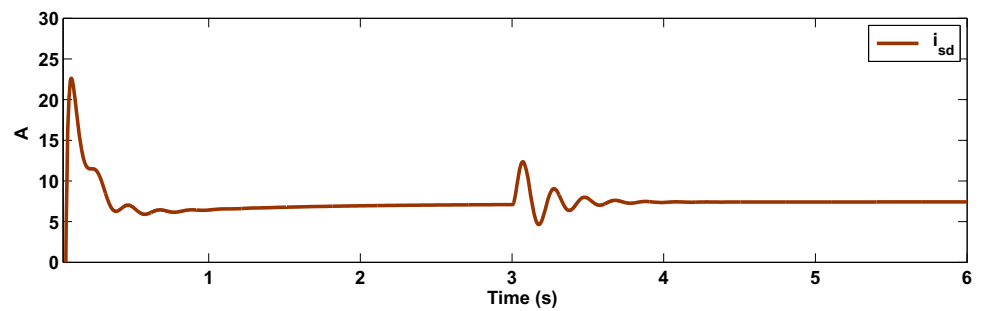


Fig. 18 Scenario 2: the stator current (quadrature component)

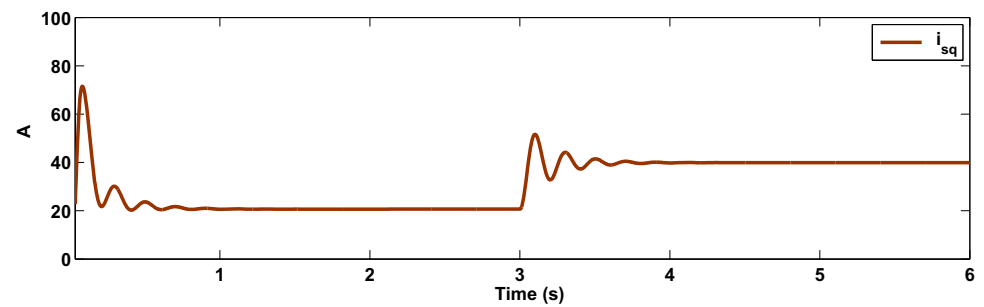


Fig. 19 Scenario 2: the control signal (V_{sd})

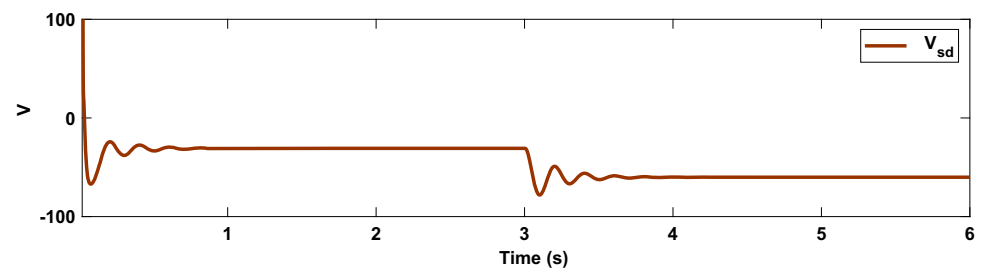


Fig. 20 Scenario 2: the control signal (V_{sq})

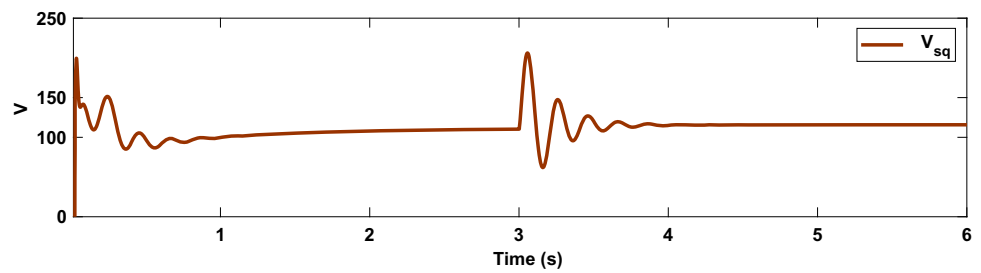


Table 3 Scenario 3: comparison of root-mean-square error in the presence of different level of measurement errors

Noise Variance	Fuzzification	Fuzzy system	\hat{e}_1	\hat{e}_2
0	Singleton	T1FS	4.877	0.057
		IT2FS	4.871	0.048
		GT2FS	4.850	0.041
	Non-singleton	T1FS	4.986	0.052
		IT2FS	4.962	0.141
		GT2FS	4.861	0.051
0.001	Singleton	T1FS	5.931	0.079
		IT2FS	5.822	0.073
		GT2FS	4.871	0.059
	Non-singleton	T1FS	5.716	0.069
		IT2FS	5.042	0.067
		GT2FS	4.868	0.057
0.05	Singleton	T1FS	7.881	0.271
		IT2FS	6.171	0.201
		GT2FS	5.975	0.174
	Non-singleton	T1FS	5.784	0.197
		IT2FS	5.235	0.138
		GT2FS	5.168	0.137

Table 4 Comparison of the root-mean-square of the tracking error for different control methods

	FTAC	FOC	T2FSC	ASMC	Proposed controller
w	39.45	46.01	40.40	35.46	4.86
ϕ	0.14	0.19	0.08	0.1	0.05

mode control technique (T2FSC) (Masumpoor and Khanesar 2015) are considered. The root-mean-square errors (RMSEs) of different control approaches are provided in Table 4. One can see that suggested method performance is more better than the other techniques. It must be taken to account that in contrary to the other approaches, the mathematical dynamics model of the IM is considered to be fully unknown in the suggested control method.

6 Conclusion

In this paper, a new robust control approach is proposed for the control of induction motors (IM) based on the generalized

type-2 fuzzy system. The dynamics of IM is unknown and is disturbed by the changes in rotor resistance and load torque. A new robust compensator is proposed to cope with approximation errors and disturbances. The type-2 fuzzy systems are optimized through the adaptation laws that are derived from Lyapunov robustness analysis. The simulations exhibit that the suggested controller has good and desired performance. Also the comparison with some other control techniques verify the strong effectiveness of the suggested control method. Furthermore, the comparison of the tracking performance of the suggested control system with other kind of fuzzy systems and fuzzification methods demonstrates that the suggested fuzzy control system has better capability in the presence of measurement errors, abrupt faults and unknown time-varying dynamics. The main limitation is that the actuator failures have not been considered. For our future studies, this problem in practical application is taken to account. .

Author contributions Akram Sedaghati contributed to Writing—original draft; formal analysis, and Naser Pariz, Mehdi Siahni and Roohollah Barzamini contributed to formal analysis, writing—review and investigation.

Funding There is no funding source for this paper.

Availability of data and material There is no data and material.

Compliance with ethical standards

Conflict of interest The authors declare that they have no conflict of interest.

Code availability There is no code.

References

- Ali ES (2015) Speed control of induction motor supplied by wind turbine via imperialist competitive algorithm. *Energy* 89:593–600
- Ammar A, Talbi B, Ameid T, Azzoug Y, Kerrache A (2019) Predictive direct torque control with reduced ripples for induction motor drive based on t–s fuzzy speed controller. *Asian J Control*. <https://doi.org/10.1002/asjc.2148>
- Boumella N, Djouani K, Boulemden M (2012) A robust interval type-2 TSK fuzzy logic system design based on chebyshev fitting. *Int J Control Autom Syst* 10(4):727–736

- Chang W-J, Lin Y-H, Du J, Chang C-M (2019) Fuzzy control with pole assignment and variance constraints for continuous-time perturbed Takagi–Sugeno fuzzy models: application to ship steering systems. *Int J Control Autom Syst* 17(10):2677–2692
- Castillo O, Atanassov K (2019) Comments on fuzzy sets, interval type-2 fuzzy sets, general type-2 fuzzy sets and intuitionistic fuzzy sets. In: *Recent advances in intuitionistic fuzzy logic systems*. Springer, Berlin, pp 35–43
- Castillo O, Melin P, Valdez F, Soria J, Ontiveros-Robles E, Peraza C, Ochoa P (2019) Shadowed type-2 fuzzy systems for dynamic parameter adaptation in harmony search and differential evolution algorithms. *Algorithms* 12(1):17
- Das A, Bera UK, Maiti M (2018) Defuzzification and application of trapezoidal type-2 fuzzy variables to green solid transportation problem. *Soft Comput* 22(7):2275–2297
- Deng W, Yao R, Zhao H, Yang X, Li G (2019) A novel intelligent diagnosis method using optimal LS-SVM with improved PSO algorithm. *Soft Comput* 23(7):2445–2462
- Dong C, Brandstetter P, Vo HH, Tran TC, Vo DH (2016) Adaptive sliding mode controller for induction motor. In: *International conference on advanced engineering theory and applications*. Springer, Berlin, pp 543–553
- Farah N, Talib MHN, Shah NSM, Abdullah Q, Ibrahim Z, Lazi JBM, Jidin A (2019) A novel self-tuning fuzzy logic controller based induction motor drive system: an experimental approach. *IEEE Access* 7:68172–68184
- Fekih A (2008) Effective fault tolerant control design for nonlinear systems: application to a class of motor control system. *IET Control Theory Appl* 2(9):762–772
- Gopal BV, Shivakumar E (2019) Design and simulation of neuro-fuzzy controller for indirect vector-controlled induction motor drive. In: *Nagabhushan P, Guru D, Shekar B, Kumar Y (eds) Data analytics and learning*. Springer, Berlin, pp 155–167
- Guazzelli PRU, de Andrade Pereira WC, de Oliveira CMR, de Castro AG, de Aguiar ML (2018) Weighting factors optimization of predictive torque control of induction motor by multiobjective genetic algorithm. *IEEE Trans Power Electron* 34(7):6628–6638
- Guedes JJ, Castoldi MF, Goedtel A, Agulhari CM, Sanches DS (2019) Differential evolution applied to line-connected induction motors stator fault identification. *Soft Comput* 23(21):11217–11226
- Jana DK, Pramanik S, Sahoo P, Mukherjee A (2019) Interval type-2 fuzzy logic and its application to occupational safety risk performance in industries. *Soft Comput* 23(2):557–567
- Jhang J-Y, Lin C-J, Lin C-T, Young K-Y (2018) Navigation control of mobile robots using an interval type-2 fuzzy controller based on dynamic-group particle swarm optimization. *Int J Control Autom Syst* 16(5):2446–2457
- Kalat AA (2019) A robust direct adaptive fuzzy control for a class of uncertain nonlinear mimo systems. *Soft Comput* 23(19):9747–9759
- Kali Y, Rodas J, Saad M, Gregor R, Benjielloun K, Doval-Gandoy J, Goodwin G (2018) Speed control of a five-phase induction motor drive using modified super-twisting algorithm. In: *International symposium on power electronics, electrical drives, automation and motion (SPEEDAM)*. IEEE, pp 938–943
- Kubota H, Matsuse K (1994) Speed sensorless field-oriented control of induction motor with rotor resistance adaptation. *IEEE Trans Ind Appl* 30(5):1219–1224
- Lascu C, Jafarzadeh S, Fadali MS, Blaabjerg F (2016) Direct torque control with feedback linearization for induction motor drives. *IEEE Trans Power Electron* 32(3):2072–2080
- Lim CS, Levi E, Jones M, Rahim NA, Hew WP (2013) FCS-MPC-based current control of a five-phase induction motor and its comparison with PI-PWM control. *IEEE Trans Ind Electron* 61(1):149–163
- Lopes TD, Goedtel A, Palácios RHC, Godoy WF, de Souza RM (2017) Bearing fault identification of three-phase induction motors bases on two current sensor strategy. *Soft Comput* 21(22):6673–6685
- Masumpoor S, Khanesar MA et al (2015) Adaptive sliding-mode type-2 neuro-fuzzy control of an induction motor. *Expert Syst Appl* 42(19):6635–6647
- Melin P, Ontiveros-Robles E, Gonzalez CI, Castro JR, Castillo O (2019) An approach for parameterized shadowed type-2 fuzzy membership functions applied in control applications. *Soft Comput* 23(11):3887–3901
- Mohammadzadeh A, Kaynak O (2019) A novel general type-2 fuzzy controller for fractional-order multi-agent systems under unknown time-varying topology. *J Frankl Inst* 356(10):5151–5171
- Mohammadzadeh A, Zhang W (2019) Dynamic programming strategy based on a type-2 fuzzy wavelet neural network. *Nonlinear Dyn* 95(2):1661–1672
- Mohammadzadeh A, Ghaemi S, Kaynak O et al (2019a) Robust predictive synchronization of uncertain fractional-order time-delayed chaotic systems. *Soft Comput* 23(16):6883–6898
- Mohammadzadeh A, Sabzalian MH, Zhang W (2019b) An interval type-3 fuzzy system and a new online fractional-order learning algorithm: theory and practice. *IEEE Trans Fuzzy Syst* 28:1940–1950
- Ontiveros-Robles E, Melin P (2020) Toward a development of general type-2 fuzzy classifiers applied in diagnosis problems through embedded type-1 fuzzy classifiers. *Soft Comput* 24(1):83–99
- Ponce P, Ponce H, Molina A (2018) Doubly fed induction generator (DFIG) wind turbine controlled by artificial organic networks. *Soft Comput* 22(9):2867–2879
- Regaya CB, Farhani F, Zaafouri A, Chaari A (2018) A novel adaptive control method for induction motor based on backstepping approach using dSpace DS 1104 control board. *Mech Syst Signal Process* 100:466–481
- Sabzalian MH, Mohammadzadeh A, Lin S, Zhang W (2019a) Robust fuzzy control for fractional-order systems with estimated fraction-order. *Nonlinear Dyn* 98(3):2375–2385
- Sabzalian MH, Mohammadzadeh A, Lin S, Zhang W (2019b) New approach to control the induction motors based on immersion and invariance technique. *IET Control Theory Appl* 13:1466–1472
- Shabaniyan M, Montazeri M (2011) A neuro-fuzzy online fault detection and diagnosis algorithm for nonlinear and dynamic systems. *Int J Control Autom Syst* 9(4):665
- Thangaraj R, Chelliah TR, Pant M, Abraham A, Grosan C (2011) Optimal gain tuning of pi speed controller in induction motor drives using particle swarm optimization. *Log J IGPL* 19(2):343–356
- Uddin MN, Radwan TS, Rahman MA (2002) Performances of fuzzy-logic-based indirect vector control for induction motor drive. *IEEE Trans Ind Appl* 38(5):1219–1225
- Ustun SV, Demirtas M (2008) Optimal tuning of pi coefficients by using fuzzy-genetic for v/f controlled induction motor. *Expert Syst Appl* 34(4):2714–2720
- Xu D, Song X, Jiang B, Yang W, Yan W (2019) Data-driven sliding mode control for mimo systems and its application on linear induction motors. *Int J Control Autom Syst* 17(7):1717–1725
- Xu D, Huang J, Su X, Shi P (2019) Adaptive command-filtered fuzzy backstepping control for linear induction motor with unknown end effect. *Inf Sci* 477:118–131
- Yu X, Dunnigan MW, Williams BW (2001) Comparative study of sliding mode speed and position control of a vector-controlled induction machine. *Trans Inst Measur Control* 23(2):83–101
- Zarandi MF, Soltanzadeh S, Mohammadi A, Castillo O (2019) Designing a general type-2 fuzzy expert system for diagnosis of depression. *Appl Soft Comput* 80:329–341
- Zina HB, Allouche M, Souissi M, Chaabane M, Chrifi-Alaoui L, Bouattour M (2018) A Takagi–Sugeno fuzzy control of induction motor drive: experimental results. *Int J Autom Control* 12(1):44–61

- Zhang Y, Yang H (2015) Two-vector-based model predictive torque control without weighting factors for induction motor drives. *IEEE Trans Power Electron* 31(2):1381–1390
- Zhang Y, Yang H, Xia B (2016) Model-predictive control of induction motor drives: torque control versus flux control. *IEEE Trans Ind Appl* 52(5):4050–4060
- Zhao Z, Yu J, Zhao L, Yu H, Lin C (2018) Adaptive fuzzy control for induction motors stochastic nonlinear systems with input saturation based on command filtering. *Inf Sci* 463:186–195
- Zhang Z, Wang T, Chen Y, Lan J (2019) Design of type-2 fuzzy logic systems based on improved ant colony optimization. *Int J Control Autom Syst* 17(2):536–544
- Zhao T, Li P, Cao J (2019) Self-organising interval type-2 fuzzy neural network with asymmetric membership functions and its application. *Soft Comput* 23(16):7215–7228

Publisher's Note Springer Nature remains neutral with regard to jurisdictional claims in published maps and institutional affiliations.